ELSEVIER

Thermochimica Acta 288 (1996) 9–27

thermochimica acta

On the determination of nucleation and growth kinetics by calorimetry

Carsten Michaelsen [a,*], Michael Dahms [b]

[a] *Institute of Materials Research, GKSS Research Center, 21502 Geesthacht, Germany*
[b] *Flensburg Polytechnical Institute, 24943 Flensburg, Germany*

Received 26 April 1996; accepted 12 June 1996

Abstract

The Johnson-Mehl-Avrami (JMA) theory for nucleation and growth transformations is applied to isothermal and non-isothermal conditions as frequently used in differential scanning calorimetry (DSC) experiments. A model is derived with three kinetic parameters: activation energy, transformation order, and frequency factor. Analytical expressions are developed for the DSC heat-flow evolution as a function of time or temperature for both isothermal as well as constant heating rate conditions. They provide a variety of methods for the determination of the three kinetic parameters by fits to experimental DSC curves. The potential of the proposed model is demonstrated using the example of solid-state reactions in a Ti-Al multilayer thin film.

Keywords: Nucleation and growth kinetics; Calorimetry; Solid-state reactions; Ti-Al; Multilayer thin films

1. Introduction

Phase transformations which take place by nucleation and growth have been analyzed in terms of the Johnson-Mehl-Avrami (JMA) theory for some fifty years with great success [1–3]. The effectiveness of this theory is based on its mathematical simplicity, which manifests itself in the high flexibility which enables the description of phase transformations for a wide variety of nucleation and growth mechanisms as well as growth morphologies.

* Corresponding author.

PII S0040-6031(96)03039-0

From an experimental viewpoint, phase transformations are frequently investigated by calorimetric methods. The significance of differential scanning calorimetry (DSC) and differential thermal analysis (DTA) stems from their straightforwardness and flexibility. For example, a DSC measurement performed at a constant heating rate enables several transformations to be identified in a single experiment by covering a wide temperature range. Furthermore, DSC measurements allow both the determination of important thermodynamic quantities, such as enthalpy differences between phases, as well as the characterization of the kinetics of the transformation considered. A well-known example for the kinetic characterization of phase transformations is the Kissinger method [4,5], which allows the determination of the activation energy E_a of a process through examination of the DSC-peak temperature shift induced by variation of the heating rate. Moreover, there is a significant number of investigations which focus on the determination of further kinetic parameters by considering not only the DSC peak temperature but also the full shape of the DSC trace obtained for various experimental conditions [6–16]. For nucleation and growth transformations, these additional kinetic parameters are a JMA exponent, n, and a rate constant, k. The JMA exponent, n, can be addressed with the time laws of nucleation and growth as well as the growth morphology, and will usually lie between 0.5 and 4. The rate constant, k, provides information about the transformation velocity and its dependence on temperature.

However, the JMA theory was developed only for isothermal conditions, while DSC measurements are most frequently performed at constant heating rate for experimental convenience. Therefore, several attempts have been made to apply the JMA theory to the conditions of constant heating rates. The validity of such modifications is limited and has been critically assessed by a number of authors [7–13]. Most of the methods so developed require numerical integration of the DSC signal in order to obtain the transformed volume fraction, X_V, as a function of time or temperature. However, such numerical integrations can be subject to systematic errors, caused for example by uncertainties about the exact course of the baseline.

In this paper, an analytical approach with three parameters is developed for the description of DSC traces which includes analysis of peak position and shape, both for the experimental conditions of constant temperatures and constant heating rates. This analytical approach allows the kinetic analysis of simple nucleation and growth transformations by fits to experimental DSC data. It will also be shown that baseline corrections, if required, can be treated by an analytical approach, thus eliminating difficulties arising with numerical or iterative data evaluation methods. The potential of the proposed theory is demonstrated using the example of two transformations which occur upon annealing of a Ti-Al multilayer thin film.

2. Mathematical description

In the following sections, analytical solutions for DSC traces will be derived for nucleation and growth transformations, for isothermal conditions as well as for the conditions of constant heating rates. We will assume that the heat flow rate, ϕ, measured in a calorimeter is proportional to the change of transformed volume fraction

X_V, so that for isothermal conditions

$$\phi = \Delta H \cdot \frac{\mathrm{d}X_V}{\mathrm{d}t}, \tag{1}$$

and for constant-heating-rate experiments

$$\phi = \Delta H \cdot \beta \cdot \frac{\mathrm{d}X_V}{\mathrm{d}T}, \tag{2}$$

where ΔH is the total enthalpy difference between the transformed and the untransformed state, and β is the heating rate. This assumption implies that only two states exist which are the untransformed and the transformed state. Further, it implies that these two states have a fixed enthalpy difference which is independent of temperature and time. This assumption will be justified in many cases, but it can be violated in special situations. For example, the enthalpy of amorphous phases is substantially temperature dependent above the glass transition temperature [17,18].

2.1. Fundamental considerations

A JMA-type transformation is the result of a combined nucleation and growth process, where nucleation takes place at random loci and the transformed volume fraction is affected by the impingement of the growing nuclei. The transformed volume fraction can be described in exponential form

$$X_V = 1 - \exp(-X_{ex}), \tag{3}$$

where X_{ex} is the extended volume fraction that would have been transformed without impingement. The extended volume fraction at time t for growth in n dimensions can be related to the geometry of the growing nuclei by

$$X_{ex}(t) = k \cdot \int_0^t I(\tau) \cdot r^n(t, \tau) \mathrm{d}\tau, \tag{4}$$

where $I(\tau)$ is the nucleation rate at time τ prior to t, $r(t, \tau)$ is the radius of a nucleus which has started to grow at time τ, and k is a geometry factor. For example, $k = (4\pi/3)$ for radial growth in three dimensions from pre-existing nuclei. In the following we will consider two cases, i.e., the case (a) where all nuclei are pre-existing, and the case (b) where nuclei are formed at a constant rate.

(a) For the case of a fixed number, N, of pre-existing nuclei per unit volume, Eq. (4) transforms to

$$X_{ex} = k_1 \cdot r^n, \tag{5}$$

with $k_1 = k \cdot N$.

The classical Avrami analysis is strictly valid only for constant growth rates which are independent of time. These linear growth kinetics can be described by an Arrhenius-Ansatz,

$$\frac{\mathrm{d}r}{\mathrm{d}t} = k_2 \cdot \exp\left(-\frac{E_a^G}{k_B T}\right), \tag{6}$$

where E_a^G is the activation energy for growth, and k_2 is a rate constant. As discussed in detail by Christian [3], the JMA formalism still provides a reasonable approximation for the early stages of the transformation when the growth is diffusion-controlled. The present model can be modified to apply to diffusion-controlled processes, by replacing $(\mathrm{d}r/\mathrm{d}t)$ by $(r\mathrm{d}r/\mathrm{d}t)$. The result of this modification is mathematically identical to the present formalism except that n is replaced by $n/2$.

(b) For the situation that nucleation takes place throughout the process at a constant rate, I, this nucleation rate is also considered to be thermally activated,

$$I = k_3 \cdot \exp\left(-\frac{E_a^N}{k_B T}\right), \tag{7}$$

where E_a^N is the activation energy for nucleation, and k_3 is another rate constant. This case has already been considered by de Bruijn et al. [10] and Woldt [11], for different activation energies of nucleation and growth and for integer values of n. The result of these earlier investigations is that the kinetics of the transformation are determined by an average activation energy which is given by $E_a = (E_a^N + nE_a^G)/(n+1)$, indicating that the two individual activation energies cannot be determined separately from kinetic analyses. Hence we will confine attention in the present paper to transformations that can be characterized by a single activation energy, by assuming $E_a^G = E_a^N = E_a$. In contrast to the work of de Bruijn et al. [10] and Woldt [11], this simplification enables us to treat the reaction order n as a continuous variable. As can be seen later, the formalism then reduces to three parameters which can be determined experimentally.

With $E_a^G = E_a^N = E_a$, combination of Eqs. (6) and (7) leads to

$$I(\tau) = \frac{k_3}{k_2} \cdot \frac{\mathrm{d}r}{\mathrm{d}t}(\tau), \tag{8}$$

which means that the nucleation rate becomes proportional to the growth rate. This proportionality is trivial for isothermal conditions where both rates are constant. For non-isothermal conditions it is the consequence of the simplification that both processes are characterized by the same activation energy. Inserting Eq. (8) into Eq. (4) leads to

$$X_{ex} = \frac{kk_3}{k_2} \cdot \int_0^t \frac{\mathrm{d}r}{\mathrm{d}\tau} r^n(t,\tau)\mathrm{d}\tau = \frac{kk_3}{k_2(n+1)} \cdot r^{n+1}(t,0) \tag{9}$$

where $r(t,0)$ is the radius of a nucleus which has started to grow at $\tau = 0$, i.e. the maximum radius.

Comparison of the Eqs. (5) and (9) shows that for both cases of constant number of pre-existing nuclei (case (a)) as well as constant nucleation rates when the activation energies for nucleation and for growth are identical (case (b)), the extended volume fraction can be written in the form of Eq. (5), where growth occurs in n or $n-1$ dimensions for case (a) or (b), respectively. Moreover, it can be shown that for the cases where formulation (5) is valid, the transformation rate is independent of thermal history, i.e., dependent only on fraction transformed and on temperature but not explicitely on time. As discussed in detail elsewhere [9,12,13], this is an essential

condition for an application to non-isothermal measurements. Using the Eqs. (3) and (5), the transformation rate can be expressed in terms of the radius r by

$$\frac{dX_V}{dt} = \frac{dX_{ex}}{dt}\exp(-X_{ex}) = nk_1 r^{n-1}\frac{dr}{dt}\exp(-k_1 r^n). \tag{10}$$

Depending on whether the DSC experiment is carried out isothermally or at constant heating rates, the differential equation (10) has different solutions which are discussed separately in the following sections.

2.2. *Isothermal experiments*

Under isothermal conditions, integration of Eq. (6) leads to

$$r = k_2 \cdot \exp\left(-\frac{E_a}{k_B T}\right)\cdot t. \tag{11}$$

With the definition of a frequency factor

$$\nu = k_2 \sqrt[n]{k_1}, \tag{12}$$

one obtains with the Eqs. (3), (5) and (11)

$$X_V = 1 - \exp\left(-\nu^n \exp\left(-\frac{nE_a}{k_B T}\right)\cdot t^n\right) \tag{13}$$

and with the Eqs. (10), (6) and (11)

$$\frac{dX_V}{dt} = n\nu^n \exp\left(-\frac{nE_a}{k_B T}\right)\cdot t^{n-1}\cdot \exp\left(-\nu^n \exp\left(-\frac{nE_a}{k_B T}\right)\cdot t^n\right). \tag{14}$$

The above equations show that the transformed volume fraction and its time derivative depend on the three parameters n, E_a, and ν. Equation (13) is equivalent to the more frequently used equation

$$X_V = 1 - \exp(-kt^n). \tag{15}$$

The time-independent prefactor k in Eq. (15) is expressed in Eq. (13) explicitly in terms of the activation energy E_a and the frequency factor ν, as

$$k = \nu^n \exp\left(-\frac{nE_a}{k_B T}\right). \tag{16}$$

It is noteworthy that the appropriate activation energy for k is nE_a, and not E_a, when k is defined as in Eq. (15). The variable t may be replaced by $(t - t_0)$ with a positive or negative value of t_0, in order to account for possible effects such as incubation times, thermal lags of the calorimeter, or initial reactions which may take place during heating to the hold temperature.

A series of isothermal DSC traces with various values of n is calculated from Eq. (14) and shown in Fig. 1. The result is equivalent to Fig. 1 in Ref [14]. Transformations with $n > 1$ display a more or less asymmetric peak, with its position progressively shifted to

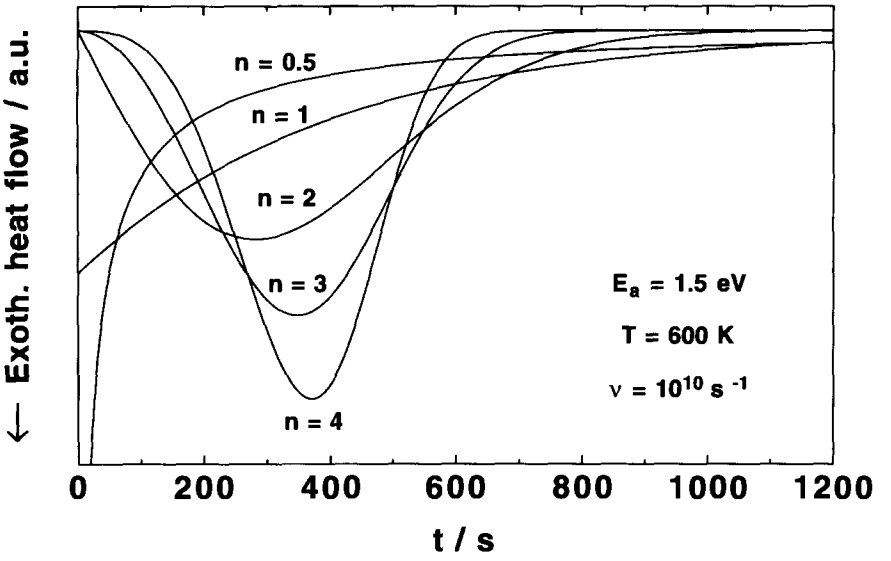

Fig. 1. Isothermal DSC traces for a temperature of 600 K and various values of n, calculated from Eq. (14) with the parameters $E_a = 1.5$ eV and $\nu = 10^{10}\ s^{-1}$.

shorter times when n is decreased, whereas transformations with $n \leq 1$ show a signal always monotonically decreasing. Hence, the reaction order n can be obtained directly from a single isothermal measurement. This is because the quantity k only affects the position of the isothermal trace but not its shape. However, k cannot be separated into the parameters ν and E_a from a single isothermal measurement. The determination of n can be carried out by an Avrami plot, from the slope of $\ln(-\ln(1-X_V))$ against $\ln t$. However, this method requires numerical integration of the isothermal DSC curve. Therefore, we will determine n not by an Avrami plot but by fits of Eq. (14) to the DSC raw data.

When a series of isothermal measurements at different temperatures is performed, a plot of $\ln k$ against $1/(k_B T)$ will yield a straight line with slope $-nE_a$. Therefore, with a knowledge of n from an Avrami plot or from a fit of the differential of Eq. (15) to the original DSC measurement, E_a can be determined. Further, it can be shown that a plot of $\ln t_{max}$ vs. $1/(k_B T)$, where t_{max} is the time when the isothermal heat flow is at maximum, gives a straight line with slope E_a. Clearly, this method to determine E_a is valid only when the isothermal trace actually exhibits a maximum, i.e. for $n > 1$. Therefore, all unknown parameters can be determined, in principle, solely from a series of isothermal measurements, including the separation of k into ν and E_a. However, as discussed later, the experimental uncertainties associated with this method to determine the activation energy will be substantially larger than those pertaining to an analysis of constant-heating-rate measurements. Therefore, this type of data evaluation will not be considered further.

2.3. Constant-heating-rate experiments

Although the JMA equation was originally developed for isothermal experiments, we will apply the theory now to experiments which are performed at constant heating rates. The validity of the application of the isothermal JMA equation under nonisothermal conditions as well as the possibility to determine the JMA exponent n and the activation energy E_a from constant-heating-rate experiments has been investigated in Refs. [7–13]. With

$$\mathrm{d}t = \frac{\mathrm{d}T}{\beta}, \tag{17}$$

the transformation rate is written as

$$\frac{\mathrm{d}X_V}{\mathrm{d}T} = nk_1 r^{n-1}\frac{\mathrm{d}r}{\mathrm{d}T}\exp(-k_1 r^n), \tag{18}$$

and the radial growth rate as

$$\frac{\mathrm{d}r}{\mathrm{d}T} = \frac{k_2}{\beta}\cdot\exp\left(-\frac{E_a}{k_B T}\right). \tag{19}$$

The differential Eq. (19) can be solved [10], leading to

$$r = \frac{k_2 k_B T^2}{\beta E_a}\exp\left(-\frac{E_a}{k_B T}\right)\cdot(1+\Delta) + r_0. \tag{20}$$

The constant r_0 is the hypothetical radius of a nucleus at $T = 0$. In the following, we assume that $r_0 = 0$. The residuum Δ depends on $((k_B T)/E_a)^i$ with $i = 1, 2, 3\ldots$. Under normal circumstances, such as temperatures below 1000 K and activation energies larger than 1 eV, it is well below 10%. More important, changes of Δ in the course of a transformation are usually well below 1%, and therefore we will neglect it. Again, with the definition of the frequency factor, ν, it follows by combination of Eqs. (3), (5) and (20) that

$$X_V \approx 1 - \exp\left[-\left(\frac{\nu}{\beta}\cdot\frac{k_B T^2}{E_a}\exp\left(-\frac{E_a}{k_B T}\right)\right)^n\right] \tag{21}$$

This expression is equivalent to Eq. (35) of Ref. [10]. However, in Ref. [10] its validity was not examined in detail.

In logarithmic form, Eq. (21) reads as

$$\ln(-\ln(1-X_V)) \approx n\cdot\ln\left(\frac{\nu}{\beta}\right) + n\cdot\ln\left(\frac{k_B T^2}{E_a}\right) - \frac{nE_a}{k_B T}. \tag{22}$$

Since the term $(k_B T^2)/E_a$ will not vary strongly compared to the exponential function $\exp(-(nE_a)/(k_B T))$, Eq. (21) is dominated by this exponential function, and a plot of $\ln(-\ln(1-X_V))$ vs. $1/(k_B T)$ will give approximately a straight line with slope $-nE_a$. Therefore, the product nE_a can be determined by numerical integration of a single constant-heating-rate scan. The error in nE_a associated with this approximation will be

of the order of 5%. However, a single constant-heating-rate measurement does not allow the separate determination of n and E_a. This conclusion is in contrast to earlier work reviewed by Henderson [9,19], which suggested a method to determine both n and E_a by a single-scan technique.

However, we will follow a different approach which avoids the errors introduced by the above approximation, as well as the errors which result from numerical integration of the DSC signal. Combination of Eqs. (18), (19) and (20) yields directly the temperature derivative of the transformed volume fraction

$$\frac{dX_V}{dT} \approx n\left(\frac{\nu}{\beta}\right)^n \exp\left(-\frac{nE_a}{k_B T}\right)\cdot\left(\frac{k_B T^2}{E_a}\right)^{n-1}\cdot\exp\left[-\left(\frac{\nu}{\beta}\right)^n \exp\left(-\frac{nE_a}{k_B T}\right)\cdot\left(\frac{k_B T^2}{E_a}\right)^n\right]. \tag{23}$$

Equation (23) is plotted in Fig. 2 for various values of n. The result is equivalent to Fig. 3 in Ref. [14]. Figure 2 indicates that, for a given value of the activation energy, n can be obtained from the width of the DSC trace, and the factor ν can be determined from the peak position. Additional simulations with other sets of parameters show that identical curves can be generated when the product nE_a is approximately constant. For example, the combination $n = 2$ and $E_a = 3$ eV gives a curve which is identical to that displayed in Fig. 2 for $n = 4$ and $E_a = 1.5$ eV. This confirms that a single scanning measurement enables the determination of nE_a, but not the separate determination of n and E_a. However, both parameter sets will then require different values of ν in order to produce identical peak temperatures.

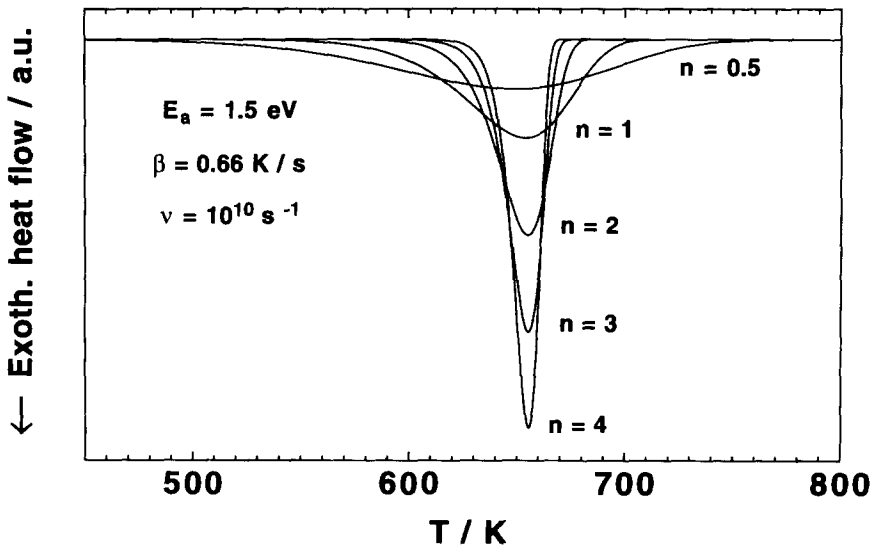

Fig. 2. Scanning DSC traces for a heating rate of 40 K/min and various values of n, calculated from Eq. (23) with the parameters $E_a = 1.5$ eV and $\nu = 10^{10}\ s^{-1}$.

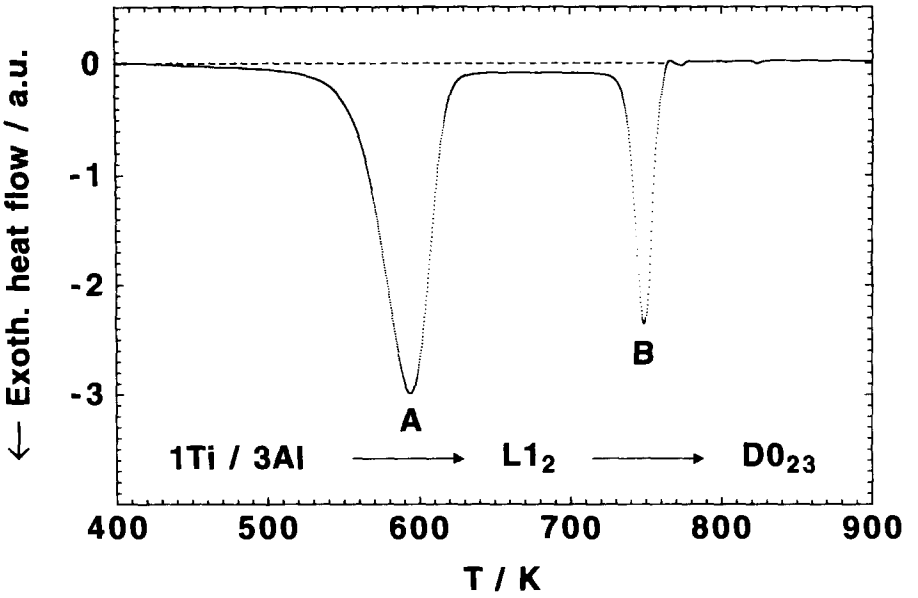

Fig. 3. Scanning DSC trace of a Ti/Al multilayer film with 1:3 molar ratio and a periodicity $\Lambda = 10$ nm, obtained at a heating rate of 40 K/min.

Proceeding now to the determination of the peak temperature, T_p, from the present theory, the derivative of the transformation rate given by Eq. (18) is set to zero. After some rearrangement, one obtains

$$((n-1)-nk_1r^n)\left(\frac{dr}{dT}\right)^2+r\frac{d^2r}{dT^2}=0. \tag{24}$$

The second derivative of the radius is

$$\frac{d^2r}{dT^2}=\frac{k_2}{\beta}\cdot\exp\left(-\frac{E_a}{k_BT}\right)\left(\frac{E_a}{k_BT^2}\right). \tag{25}$$

This leads to

$$((n-1)-nk_1r^n)\frac{k_2}{\beta}\cdot\exp\left(-\frac{E_a}{k_BT_p}\right)+r\left(\frac{E_a}{k_BT_p^2}\right)=0. \tag{26}$$

Introducing the solution for $r(T)$, Eq. (20), and considering $((2k_BT)/E_a)\ll 1$, one obtains an equation of the Kissinger type:

$$\ln\left(\frac{\beta}{T_p^2}\right)\approx\ln\left(\nu\frac{k_B}{E_a}\right)-\frac{E_a}{k_BT_p}. \tag{27}$$

Hence the activation energy E_a and the frequency factor ν can be determined using the Kissinger analysis. The errors using this type of equation are 5% at maximum, as discussed in Ref. [8].

The above results provide a procedure for the determination of the kinetic parameters from constant-heating-rate measurements which has already been suggested by Criado and Ortega [8]. Firstly, a series of scanning measurements with various heating rates has to be performed. This allows the determination of the activation energy and the frequency factor following Eq. (27). Secondly, with E_a and v being determined, the remaining unknown parameter n can be obtained by a fit of Eq. (23) to a single constant-heating-rate measurement, so that all parameters are determined. Further, this fit procedure can be applied to all scanning measurements, in order to test the consistency of the parameter set. Since the fit is sensitive to the product nE_a only, the experimental error in the determination of E_a is linearly transferred to the error in n. Therefore, the precision of this method to determine n depends critically on the accuracy with which the Kissinger analysis has been performed.

3. Application to Ti-Al thin film reactions

The above methods are applied in the following sections to the kinetics of solid-state reactions in Ti/Al multilayer thin films. The multilayer films with 1 : 3 molar ratio and periodicity $\Lambda = 10$ nm were prepared by sputtering under high-purity conditions from elemental targets. DSC measurements on free-standing films were performed in a Perkin Elmer DSC 2C, equipped with a MC^2 Thermal Systems computer interface. The calorimeter was calibrated including thermal-lag corrections at various heating rates using a number of well-known transformations occurring in standard reference materials. A more detailed description of the experimental methods is given elsewhere [20–22].

A DSC trace obtained from such a multilayer sample is shown in Fig. 3. The measurement shows that two transformations can be identified. X-ray diffraction measurements taken at various stages of the DSC trace reveal that actually three transformations take place in the sample. Firstly, the DSC peak A at about 600 K is due to the solid-state reaction of the elemental multilayer, resulting in the formation of $TiAl_3$ with a metastable $L1_2$ structure. Secondly, the DSC peak B at about 750 K can be identified with a transformation of the $L1_2$ phase into $TiAl_3$ with a $D0_{23}$ structure, which is also a metastable modification. Finally, the $D0_{23}$ phase transforms into the equilibrium $D0_{22}$ structure of $TiAl_3$ between 800 and 1000K, without significant heat release.

The solid-state reactions in multilayer films are a topic under investigation in our group, so that data of good quality were available. The Ti/Al multilayer film was chosen as a model system, since it exhibits two nucleation and growth transformations with rather different character in a single sample, as will be seen in the course of the following sections. In addition, this sample shows a variety of problems as they may frequently occur in kinetic analyses of DSC measurements. Examples are baseline changes in the constant-heating-rate scans, the small temperature window available for isothermal measurements, and reactions which may already occur during heatup to the isothermal temperature. As will be shown, particularly the reaction A which is characterized by a relatively small Avrami exponent, demonstrates the occurrence of

such problems, and it indicates how these difficulties can be overcome using non-isothermal methods. It is noted that it is not a priori clear whether a transformation such as the product-phase formation in an elemental multilayer film, which gives rise to DSC peak A, is of the JMA type. This is because the JMA theory is based on the assumption of a random spatial distribution of nucleation sites, a condition which may be violated in the present case. Further, it is an open question as to whether nucleation is required at all for the first-phase formation in the presence of a very large driving force of several tens of kJ/mol. However, there are a number of recent investigations which indicate that the transformation considered can be interpreted as a nucleation and growth transformation (see Refs. [20–24] and references given therein). This problem will not be discussed further in the present paper, but is the subject of other publications. Rather, the Ti–Al multilayer sample will be treated as an arbitrary model system which allows the application of the method described above to be demonstrated. The methods will at first be applied to measurements performed at constant heating rates, and the results will then be compared to those obtained from isothermal experiments.

3.1. Constant-heating-rate experiments

DSC scans such as shown in Fig. 3 were measured at various heating rates, and the resulting peak temperatures are shown in Fig. 4 as a Kissinger plot. From the slope of the straight lines, the activation energies are determined as 1.54 ± 0.05 eV and 2.19 ± 0.16 eV for peaks A and B, respectively. Further, the intercept with the vertical axis allows the determination of the frequency factor ν by using Eq. (27). We obtain $\nu_A = 3.76 \times 10^{11}\ \mathrm{s}^{-1}$ and $\nu_B = 1.46 \times 10^{13}\ \mathrm{s}^{-1}$ for peaks A and B, respectively. For arbitrary values of n, DSC traces computed with these values of E_a and ν already produce a perfect matching with the experimental peak position temperatures T_p for all heating rates. The remaining parameter n can now be determined from the width of the DSC traces, by a fit of Eq. (23) to a single constant-heating-rate scan. Furthermore, the frequency factor may be re-determined by fit to a single scanning trace as well. Before doing so, the ability of the proposed model to correct possible changes of the baseline, which may occur in the course of the transformation considered, is briefly discussed.

Inspection of the DSC spectrum shown in Fig. 3 reveals that the baseline changes during both reactions, so that the DSC signal does not reach its initial value after reaction A. Such baseline changes may have various origins. Possible reasons are specific heat differences between untransformed and transformed sample, or irreversible reactions which may take place prior to or after the transformation, such as relaxation, strain relief or grain growth. For the correction of such a baseline change, an iterative procedure has been suggested in Ref. [16]. However, the analytical expression (21) for the transformed volume fraction allows a possible baseline correction to be incorporated into the fitting function. With the assumption that the relative baseline change is proportional to the transformed volume fraction, the baseline can be expressed by

$$\text{baseline} = b_-(1 - X_V) + b_+ X_V, \tag{28}$$

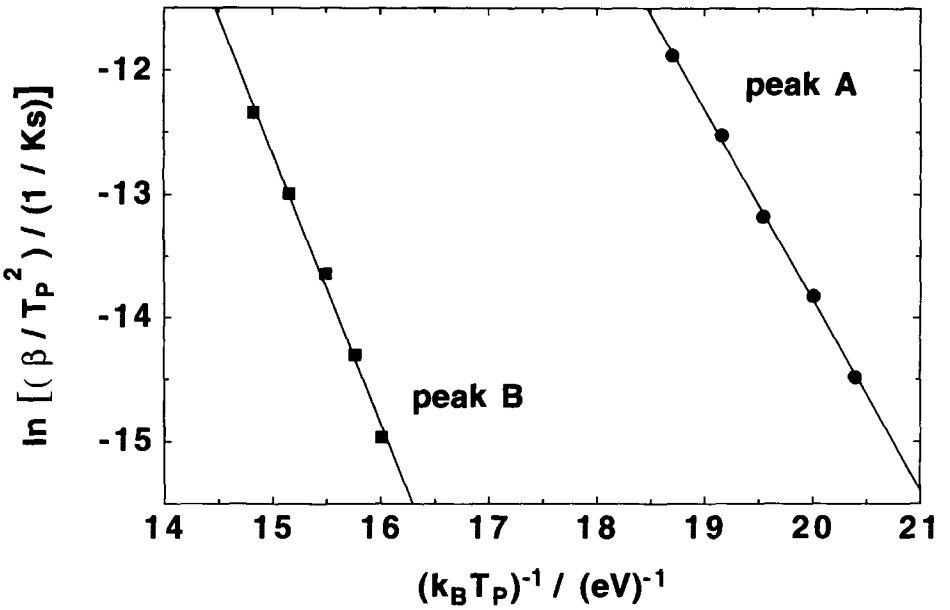

Fig. 4. Kissinger plot of the peak-temperature variation with heating rate, for the transformations A and B of a Ti/Al multilayer film with 1:3 molar ratio and a periodicity $\Lambda = 10$ nm.

where b_- and b_+ are the baselines prior to and after the transformation, respectively. Eq. (28) can be added to Eq. (23), and the resulting function can be fitted to the DSC traces.

This fitting procedure was applied to the constant-heating-rate measurements in order to obtain the reaction constant n. Figure 5 shows the DSC trace and the fitting result for a heating rate of 40 K/min. For the evaluation, the activation energies of both peaks were kept fixed as they were determined from the Kissinger analysis, and the frequency factors were re-determined by a fit to the scanning trace, taking the values obtained by the Kissinger method as starting values. Figure 5 shows that the model provides a good description of the experimental curve. Table 1 summarizes the corresponding results obtained for other heating rates. The evaluation shows that the JMA exponents n are approximately 1.3 for peak A and 3.9 for peak B. Inspection of Table 1 indicates that the n values are basically unaffected by a change in the heating rate. Also, the frequency factors do not show strong variation with changes in the heating rate, and they are in good agreement with the Kissinger method values. These results indicate that a consistent set of parameters is obtained which is able to reproduce the complete DSC traces at all heating rates.

With the kinetic parameters determined from constant-heating-rate experiments, the isothermal measurements can be predicted. In the following section, this parameter set will be compared to that determined by isothermal DSC measurements.

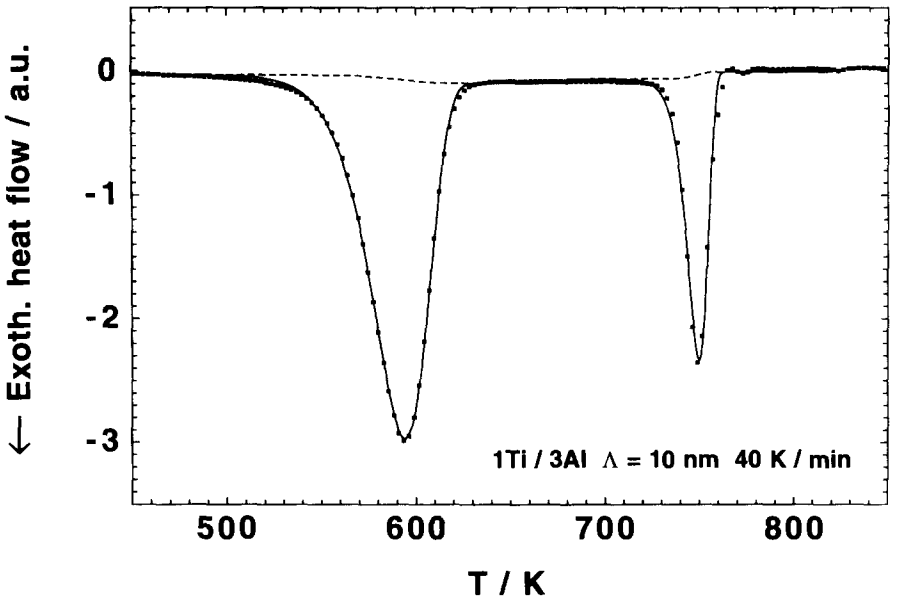

Fig. 5. Scanning DSC trace of a Ti/Al multilayer film with 1:3 molar ratio and a periodicity $\Lambda = 10$ nm, obtained at a heating rate of 40 K/min. Only every tenth data point is plotted for better visibility. The solid line is the fit to the measurement and the broken line indicates the baseline change, as described in the text.

Table 1
Kinetic parameters n_A, ν_A, and n_B, ν_B, for DSC peaks A and B, respectively, determined from constant-heating-rate measurements. The value in brackets has not been used for the determination of the average value.

β/K/min	n_A	$\nu_A/10^{11}\ s^{-1}$	n_B	$\nu_B/10^{13}\ s^{-1}$
10	1.29	3.70	3.86	1.36
20	1.33	3.94	3.97	1.54
40	1.30	3.76	3.92	1.64
80	1.32	3.94	3.75	1.49
160	1.28	3.72	(3.12)	1.34
average	1.30	3.81	3.88	1.47
Kissinger	–	3.76	–	1.46

3.2. *Isothermal measurements*

Although the above method allows the determination of the kinetic parameters solely from constant-heating-rate experiments as long as the proposed model is applicable, one may wish to perform additional isothermal measurements in order to test the validity of the parameter set obtained. For example, the method to determine n and E_a separately from a number of constant-heating-rate experiments may be of limited precision in some cases. In contrast, an unambiguous determination of n can be

obtained separately from a single isothermal measurement. However, such isothermal measurements have some practical disadvantages which appear to be bypassed in an experiment in which the temperature is monotonically increased, and which will be briefly discussed here.

(1) Thermal lag: When the calorimeter temperature is changed, the actual sample temperature will generally follow the desired temperature-time program in an imperfect way, giving rise to a thermal lag. For the condition of constant-heating rate, this thermal lag is expected to be a monotonic function of temperature and heating rate. Therefore, it can be corrected by measurements on a number of well-known calibration substances performed at various heating rates. For isothermal conditions, the actual sample temperature will approach the desired hold temperature exponentially with an unknown time constant. This time constant is difficult to correct for, and it may be considered as a time offset t_0 which can be introduced into Eq. (14).

(2) Small signal: In an isothermal measurement performed in a calorimeter of type DSC 2, the calorimeter typically requires 10–20 s to stabilize when it is heated at 20 K/min to the hold temperature. Therefore, an isothermal DSC measurement will normally be carried out on a time scale of 1–3 orders of magnitude larger than this value, i.e. within about 10^2–10^4 s. As a consequence, the DSC signal in an isothermal measurement is typically 1–3 orders of magnitude smaller than in a corresponding constant-heating-rate experiment, since it is distributed over a substantially wider time interval. This makes isothermal DSC measurements more difficult than constant-heating-rate measurements, and it places higher demands on the long-time stability of the calorimeter. Also, the signal expected in an isothermal measurement will be too small for a heat-flow calorimeter, but will require a power-compensated calorimeter which has a higher sensitivity but also an upper temperature limit of 1000 K.

(3) Small temperature window: Transformations which take place by nucleation and growth are thermally activated processes which have an exponential temperature dependence. Therefore, due to the limited experimental time window of about 10^2–10^4 s, the choice of the hold temperature is substantially constrained and lies typically within a window of only 20 K. This narrow temperature window available for isothermal DSC measurements is a problem which becomes more serious with decreasing value of n. For a small n value, the DSC peak of a constant-heating-rate scan can have a width substantially larger than this temperature window, and it becomes impossible to avoid initial reactions during heating to the hold temperature. Consequently, an initial peak in the isothermal trace may fall into the thermal-lag regime or will even be bypassed completely. As a consequence, only the decaying portion of the trace will be detected, and the data evaluation will incorrectly yield $n \leq 1$.

To conclude, isothermal DSC measurements have the advantage that they allow the determination of the reaction order n from a single measurement. However, they also have a number of drawbacks which are circumvented in constant-heating-rate experiments, emphasizing the significance of the proposed method which facilitates the determination of n from constant-heating-rate measurements.

The isothermal DSC measurements were performed by heating to the desired temperature at a rate of 20 K/min, and then holding the temperature until the signal

showed no further change. By repeating the measurement under identical conditions, the baseline was established which was always perfectly horizontal. Typical isothermal DSC traces obtained from transformations A and B are shown in Figs. 6 and 7, respectively. A comparison of the two measurements demonstrates the different character of these two reactions.

For the transformation A, the DSC signal revealed that the reaction had already started during heatup to the hold temperature, indicating that the subsequent isothermal measurements were taken from initially transformed samples. As can be seen from Fig. 6, the isothermal traces taken from transformation A exhibit a small peak at the initial part of the trace followed by a long decaying tail. Both features are typical of a transformation with n slightly larger than one, consistent with the result obtained from the constant-heating-rate experiments. The evaluation of the isothermal measurements was performed by fitting Eq. (14) to the data points. Again, the activation energy was kept fixed as determined from the Kissinger analysis, and the frequency factor ν and the JMA exponent n were determined by fits to the isothermal traces, taking the values obtained from the constant-heating-rate measurements as starting values. Figure 6 shows that the fit of Eq. (14) provides a good description of the decaying part of the measurement, while there is less good agreement around the initial part of the measurement. The resulting kinetic parameters are $n_A = 1.10$ and $\nu_A = 3.10 \times 10^{11}\ s^{-1}$ for the temperature of 530 K, in reasonable agreement with the values deduced from the constant-heating-rate measurements. Another possible way to

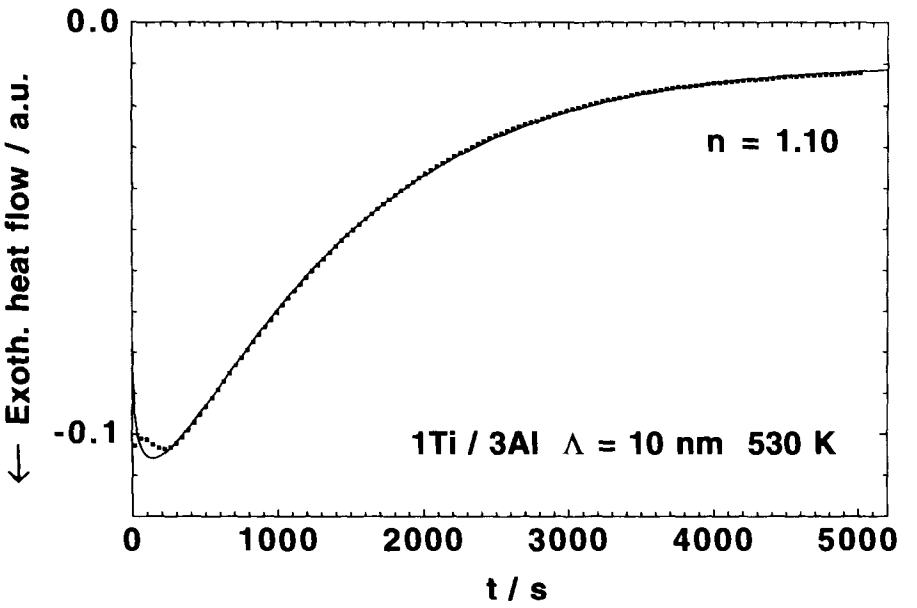

Fig. 6. Isothermal DSC trace of transformation A at a temperature of 530 K, obtained from a Ti/Al multilayer film with 1:3 molar ratio and a periodicity $\Lambda = 10$ nm. The solid line is the best fit of Eq. (14) to the measurement, as described in the text.

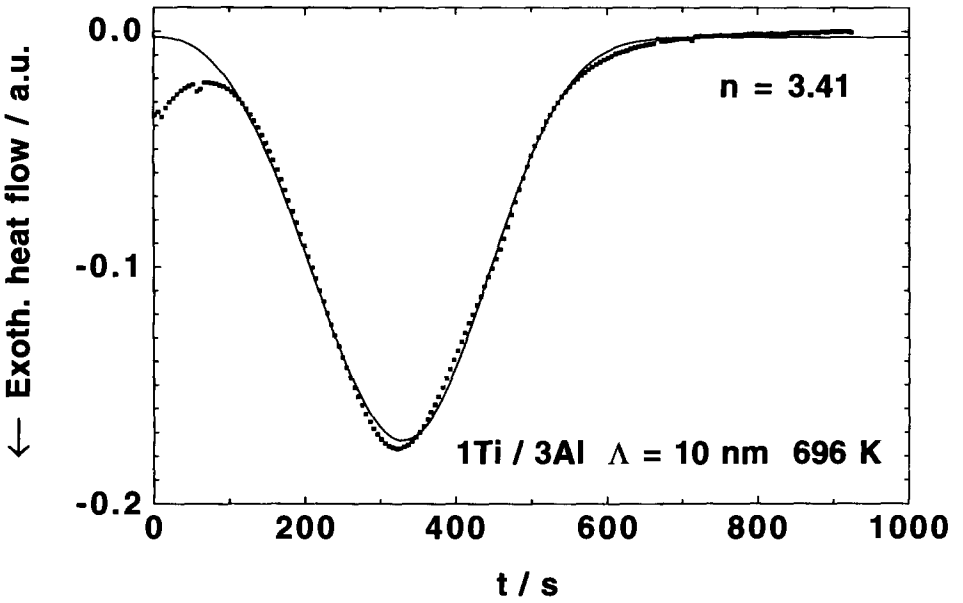

Fig. 7. Isothermal DSC trace of transformation B at a temperature of 696 K, obtained from a Ti/Al multilayer film with 1:3 molar ratio and a periodicity $\Lambda = 10$ nm. The solid line is the best fit of Eq. (14) to the measurement, as described in the text.

evaluate the isothermal measurements is to keep v fixed as it comes out of the constant-heating-rate experiments, and to re-determine E_a in addition to n. The activation energy thus determined is in excellent agreement with that obtained by the Kissinger method, with scatter upon variation of the temperature which lies within the experimental error determined from the Kissinger plot, demonstrating the consistency of the parameter set. When a (negative) time offset is incorporated into the fit in order to account for the initial transformation during heatup, the fit quality is slightly improved and the resulting n is increased towards the value obtained from the constant-heating-rate measurements, as expected from the above discussion.

For transformation B, the DSC signal again revealed that some reaction had taken place during heatup to the hold temperature. This initial heat flow can be associated with the baseline change between both reactions observed in the constant-heating-rate scans, indicating that this baseline change is of irreversible nature. This reaction also gives rise to a decaying DSC signal at the beginning of the isothermal trace, as can be seen in Fig. 7. Such a heat flow decaying with time is indicative of grain growth or ordering in the $L1_2$ phase prior to its transformation to the $D0_{23}$ phase [14,15]. The major portion of the isothermal measurement shows a bell-shaped peak typical of a JMA transformation with exponent n significantly larger than 1. Evaluation of the measurement by the method described above results in $n_B = 3.41$ and $v_B = 1.94 \times 10^{13}\ s^{-1}$ for the temperature of 696 K.

The results obtained for other temperatures are summarized in Table 2. The JMA exponents derived are approximately 1 for peak A, and lie between 3 and 4 for peak B.

Table 2
Kinetic parameters n_A, ν_A, and n_B, ν_B, for the transformations A and B, respectively, determined from isothermal measurements. The evaluation was performed without considering possible time offsets

T/K	n_A	$\nu_A/10^{11}\ s^{-1}$	n_B	$\nu_B/10^{13}\ s^{-1}$
520	1.05	1.94	–	–
530	1.10	3.10	–	–
540	1.01	2.29	–	–
676	–	–	3.34	1.45
686	–	–	3.37	1.35
696	–	–	3.41	1.94
average	1.05	2.44	3.37	1.58

Both figures are in good agreement with those obtained from the constant-heating-rate measurements, although the latter values are systematically larger by some 10–20%. Also, the frequency factors obtained from both types of measurement are approximately identical. Furthermore, inspection of Table 2 reveals that no systematic variation of ν with temperature occurs. A systematic variation of ν with temperature would indicate that the input value of the activation energy E_a deviates significantly from the true value. The absence of such a systematic variation therefore confirms the consistency of the parameter set.

The deviation of n determined from the constant-heating-rate measurements compared to the isothermal measurements of some 10–20% may have various reasons. Firstly, a systematic error of about 5% may arise from the approximations made during the mathematical deduction of the Kissinger equation, as well as other approximations introduced during the mathematical treatment of the constant-heating-rate scans. On the other hand, systematic errors may arise in the evaluation of isothermal measurements, due to possible effects such as thermal delay of the sample or initial reactions which cannot be avoided during heatup. In addition, it is possible that the three parameters which are assumed to be constant in the treatment, are not completely independent of temperature and time. Also, the assumption that nucleation and growth have identical activation energies may be a quite inexact approximation. However, none of the experiments clearly reveals the significance of two activation energies as would be required in a more general treatment. Finally, it may be possible that the Ti-Al thin-film sample is not the most appropriate choice to test the validity of the method, since both transformations investigated may be affected by the limited geometry or by the violation of some assumptions which present the basis of the JMA theory, such as the randomness of the spatial distribution of nucleation sites. Therefore, we consider the experimental uncertainty of about 10–20% for the determination of n to be of acceptable precision.

4. Conclusions

The treatment presented in this paper provides a three-parameter method for the analysis of nucleation and growth transformations, by a series of DSC measure-

ments. The main feature is that all equations are given in an analytical form, allowing the determination of the unknown parameters by fits to experimental data without the requirement of numerical integration. The parameters which are activation energy, E_a, frequency factor, v, and transformation type parameter, n, can be determined by various types of analysis, by consideration of peak position and shape both for isothermal and non-isothermal experimental conditions in a consistent way. The most convenient method to determine these parameters is to use a minimum of two constant-heating-rate scans. This method allows calculation of the activation energy and the frequency factor using the Kissinger plot. Subsequently, the remaining unknown quantity n can be obtained by a fit of Eq. (23) to a single scanning trace. This method circumvents the requirement to perform an isothermal measurement in order to obtain n, thus bypassing the experimental problems arising with isothermal measurements. However, other procedures are also possible. For example, n can be determined from a single isothermal measurement, and then the two remaining unknown parameters can be obtained by a fit of Eq. (23) to a single scanning trace.

Besides the classical Avrami-plot method to determine the JMA exponent n from an isothermal measurement, or the Kissinger method to obtain the activation energy E_a of the transformation, it appears that most of the equations contain the product of both quantities, i.e. nE_a. The key problem thus is to separate both parameters with acceptable precision. For example, the separation of both values using a number of constant-heating-rate experiments critically depends on the precision with which the activation energy of the process has been determined, besides the systematic errors introduced by the development of the Kissinger equation. On the other hand, when nE_a has been obtained from a single constant-heating-rate measurement, its separation is possible in principle via the determination of n from a single isothermal experiment. The quality of the nE_a separation then critically depends on the determination of n, which may be of limited precision due to experimental difficulties associated with thermal lags or initial reactions which occur during heatup. Furthermore, the separate determination of E_a from a number of isothermal measurements performed at various temperatures is constrained by the small temperature window available for such experiments. Since these experimental difficulties are bypassed in a continuous heating experiment, such continuous experiments may be advantageous for the determination of the kinetic parameters.

The potential of the theory is demonstrated using the example of the solid-state reaction of a Ti-Al multilayer film. It is shown that all types of measurement can be consistently described by a single set of three parameters with reasonable precision. This indicates that such a three-parameter model may be sufficient to characterize many nucleation and growth transformations.

Acknowledgements

We are grateful to K. Barmak for drawing our attention to the exciting field of studying thin-film reactions by calorimetry and for continuous stimulating discussions.

We also thank P.A. Beaven for reading the manuscript. We acknowledge the cooperative agreement No.V9480 between GKSS Research Center and Flensburg Polytechnical Institute.

References

[1] W.A. Johnson and R.F. Mehl, Trans. Am. Inst. Min. Eng., 135 (1939) 1.
[2] M. Avrami, J. Chem. Phys., 7 (1939) 1103; 8 (1940) 212; 9 (1941) 177.
[3] J.W. Christian, The Theory of Transformations in Metals and Alloys, Part I Equilibrium and General Kinetic Theory, Pergamon, Oxford, 1975.
[4] H.E. Kissinger, J. Res. Nat. Bur. Std., 57 (1956) 217; Anal. Chem., 29 (1957) 1702.
[5] J.W. Graydon, D.J. Thorpe and D.W. Kirk, Acta metall. mater., 42 (1994) 3163.
[6] A.L. Greer, Acta metall., 30 (1982) 171.
[7] L.V. Meisel and P.J. Cote, Acta metall., 31 (1983) 1053.
[8] J.M. Criado and A. Ortega, Acta metall., 35 (1987) 1715.
[9] D.W. Henderson, J. Non-Cryst. Solids, 30 (1979) 301.
[10] T. J.W. de Bruijn, W.A. de Jong and P.J. van den Berg, Thermochim. Acta, 45 (1981) 315.
[11] E. Woldt, J. Phys. Chem. Solids, 53 (1992) 521.
[12] R. Chen and Y. Kirsh, Analysis of Thermally Stimulated Processes, Pergamon, Oxford, 1981.
[13] J. Sestak, Thermophysical Properties of Solids, Thermal Analysis, Vol. XII, Elsevier, Amsterdam, 1984.
[14] L.C. Chen and F. Spaepen, J. Appl. Phys., 69 (1991) 679.
[15] L.C. Chen and F. Spaepen, Nature, 336 (1988) 366.
[16] M.G. Scott and P. Ramachandrarao, Mater. Sci. Eng., 29 (1977) 137.
[17] R. Bormann and K. Zöltzer, phys. stat. sol. (a), 131 (1992) 691.
[18] R. Bormann, Mater. Sci. Eng., A178 (1994) 55.
[19] The single-scan technique given by Henderson [9] in fact gives straight lines when $\ln(\mathrm{d}X_V/\mathrm{d}T)$ is plotted versus $1/(k_B T)$, or when $\ln(-\ln(1-X_V))$ is plotted versus $1/(k_B T)$. Henderson has concluded that the first type of plot will give a slope $-E_a$, and the second type of plot will give a slope $-nE_a$. However, we conclude that the slope is $-nE_a$ in both cases. For the first type of plot, this can be deduced from our Eq. (23). In this case, the evaluation only considers the initial portion of the transformation, before impingement becomes significant (initial rise method, Ref. [12]). For the second type of plot, the treatment corresponds to our Eq. (22).
[20] C. Michaelsen, S. Wöhlert and R. Bormann, Mat. Res. Soc. Symp. Proc., 343 (1994) 205.
[21] K. Barmak, C. Michaelsen and G. Lucadamo, submitted to J. Mater. Res., 1996.
[22] C. Michaelsen, S. Wöhlert, R. Bormann and K. Barmak, Mat. Res. Soc. Symp. Proc., 398 (1996) in print.
[23] K.R. Coffey, L.A. Clevenger, K. Barmak, D.A. Rudman and C.V. Thompson, Appl. Phys. Lett., 55 (1989) 852.
[24] E. Ma, C.V. Thompson and L.A. Clevenger, J. Appl. Phys., 69 (1991) 2211.